Received February 7, 2021, accepted February 14, 2021. Date of publication xxxx 00, 0000, date of current version xxxx 00, 0000.

Digital Object Identifier 10.1109/ACCESS.2021.3060044

Extended Dissipativity and Non-Fragile Synchronization for Recurrent Neural Networks With Multiple Time-Varying Delays via Sampled-Data Control

R. ANBUVITHYA[1], S. DHEEPIKA SRI[1], R. VADIVEL[2], NALLAPPAN GUNASEKARAN[3], AND PORPATTAMA HAMMACHUKIATTIKUL[2]

[1]Department of Mathematics, Sri Sarada College for Women (Autonomous), Salem 636016, India
[2]Department of Mathematics, Faculty of Science and Technology, Phuket Rajabhat University, Phuket 83000, Thailand
[3]Computational Intelligence Laboratory, Department of Advanced Science and Technology, Toyota Technological Institute, Nagoya 468-8511, Japan

Corresponding authors: R. Vadivel (vadivelsr@yahoo.com) and Porpattama Hammachukiattikul (porpattama@pkru.ac.th)

The work of R. Vadivel and Porpattama Hammachukiattikul was supported by the Phuket Rajabhat University, Phuket, Thailand.

ABSTRACT This paper deals with the extended dissipativity and non-fragile synchronization of delayed recurrent neural networks (RNNs) with multiple time-varying delays and sampled-data control. A suitable Lyapunov-Krasovskii Functional (LKF) is built up to prove the quadratically stable and extended dissipativity condition of delayed RNNs using Jensen inequality and limited Bessel-Legendre inequality approaches. A non-fragile sampled-data approach is applied to investigate the problem of neural networks with multiple time-varying delays, which ensures that the master system synchronizes with the slave system and is designed with respect to the solutions of Linear Matrix Inequalities (LMIs). The effectiveness of the suggested approach is established by providing suitable simulations using MATLAB LMI control toolbox. Finally, numerical examples and comparative results are provided to illustrate the adequacy of the planned control scheme.

INDEX TERMS Dissipative analysis, multiple time-varying delay, recurrent neural networks, synchronization, sampled-data control.

I. INTRODUCTION

Neural Networks (NNs) provide an interesting pattern for a wider extent of complex systems over the past few decades. Owing to its large number of applications in different areas like associative memory, parallel processing, pattern classification, moving object speed detection, optimization, etc., Recurrent neural networks (RNNs) have been comprehensively deliberated by researchers around the globe [1]–[3]. Time-delays have been undeniably engaged in the utilization of RNNs. Thus, in both theoretical and practical sense, it is however significant to emphasize the stability of delayed neural networks [4]–[8]. Moreover, it is evident that there are many important findings on stability which have been derived in the Lyapunov perspective [9]–[12].

Most of the research works have concentrated on dynamics analysis problems for RNNs. It covers topics like synchronization [13]–[15], state estimation [16], dissipativity [17], [18], stability analysis [19], and so on. Asymptotical stability of RNNs with mixed time-varying delays has been studied in [19]. The authors in [20] addressed the problem of sampled-data control for fuzzy Markovian jump systems with actuator saturation.

On the other hand, the active research area of synchronization is fascinating and it is a remarkable one in numerous real-time systems. The synchronization has a large number of engineering background like biological model framework [13], [21]–[25]. A set of new sufficient conditions ensuring the finite time synchronization of memristor based chaotic NNs has been obtained in [13]. An exponential H_∞ synchronization for a class of master and slave neural networks with norm-bounded uncertainties have been taken into consideration in [22]. Recently, in [23], the idea of random

The associate editor coordinating the review of this manuscript and approving it for publication was Haibin Sun.

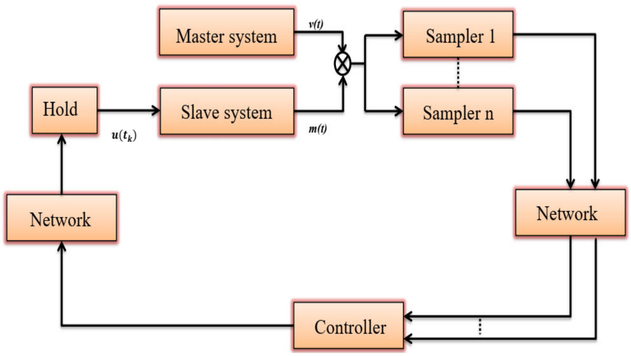

FIGURE 1. **The diagrammatic representation of master-slave sampled-data control.**

uncertainty for stochastic discrete-time systems has been proposed.

Sampled-data control technique in the field of engineering has received intensive recognition for its reliability and reliable performance compared to other control methods [26]. The idea of reliable asynchronous sampled-data filtering of T-S fuzzy uncertain delayed neural networks with stochastic switched topologies has been considered in [27]. The dissipativity theory has been used for the development and study of control systems that rely on energy-related factors [28], [29]. Furthermore, it includes H_∞ and $L_2 - L_\infty$ performance, passivity, and dissipativity performance by using new appropriate weight matrices in a performance index. Hence, it is justifiable to consider this framework for RNNs. In many of the practical situations, it is shown that the existence of small uncertainties in controllers during their design could also make closed-loop systems unstable, and such controllers are often called as fragile. It is therefore necessary to consider a robust controller for the sampled data system that ensures the closed-loop system stability and performance level when the controller gains change in the predefined admissible range [30]. Different from most of the published works, the problem of non-fragile synchronization for extended dissipativity and sampled-data RNNs with multiple time-varying delays are studied here. The structure of non-fragile sampled-data control has been represented in Fig. 1.

In view of the above discussion, the LMI based approach is developed in this paper to examine a class of RNNs with multiple time-varying delays. The main contributions and novelty of this paper are summarised as follows: (1)The quadratic stability and extended dissipativity of RNNs with multiple time-varying delays are obtained.

(2) A non-fragile synchronization is addressed for RNNs and is utilized with some novel inequalties.

(3) The desired non-fragile sampled-data controller for the considered system can be obtained with respect to a new set of LMIs utilizing MATLAB toolbox.

(4) Finally, numerical examples and comparative results are provided to illustrate the adequacy of the planned control scheme.

The structure of the paper is outlined as follows: A brief model description of RNNs and preliminaries are presented in Section II. In Section III, some main results and adequate conditions which are utilized to determine the controller gains are given. To exhibit the applicability of the proposed model, the numerical simulations are given in Section IV. In Section V, the concluding part has been given.

A. NOTATIONS

In this paper, $\mathbb{R}^n$ denotes the n-dimensional Euclidean space and the set of all $m \times n$ real matrices is denoted by $\mathbb{R}^{m\times n}$. I and 0 denote the identity and zero matrices respectively, with appropriate dimensions, asterisk $\star$ represents the symmetric term of the matrix. Moreover, the block diagonal matrix is given by $\text{diag}(\cdots)$. We define $\text{sym}(Y) = Y + Y^T$, for any square matrix $Y \in \mathbb{R}^n$. The notation A^T represents the transpose of the matrix A.

II. PRELIMINARIES

Consider the recurrent neural networks with multiple time-varying delays as follows

$$\dot{v}(t) = -Mv(t) + Cf(v(t)) + \textstyle\sum_{j=1}^{N} W_j f(v(t-\hat{\tau}_j(t))) + V(t), \tag{1}$$

where $v(t) = [v_1(t), v_2(t), \cdots, v_n(t)]^T \in \mathbb{R}^n$ represents the neuron state vector, n represents number of neurons, $f(\cdot) = [f_1(\cdot), f_2(\cdot), \cdots, f_n(\cdot)]^T \in \mathbb{R}^n$ represents the neuron activation functions, and $v(t-\hat{\tau}_j(t)) = \left[v(t-\hat{\tau}_{j1}(t)), v(t-\hat{\tau}_{j2}(t)), \cdots, v(t-\hat{\tau}_{jn}(t))\right]^T$, $v(t-\hat{\tau}_{j\hat{k}}(t)) \geq 0, j = 1, 2, \cdots, N, \hat{k} = 1, 2, \cdots, n$ denotes the time-varying delays; $M = \text{diag}(a_1, a_2, \cdots, a_n) > 0$; C, W_j denotes the connection weight $n \times n$ matrix and delayed connection weight $n \times n$ matrices respectively; $V(t) = [V_1(t), V_2(t), \cdots, V_n(t)] \in \mathbb{R}^n$ represents the external input vector.

Furthermore, the following inequality is satisfied by the neuron activation functions $f_{\hat{k}}(\cdot)$.

$$s_{\hat{k}}^- \leq \frac{f_{\hat{k}}(x_1) - f_{\hat{k}}(x_2)}{x_1 - x_2} \leq s_{\hat{k}}^+, \tag{2}$$

where $s_{\hat{k}}^-$ and $s_{\hat{k}}^+$ are constants, $x_1, x_2 \in \mathbb{R}$, $x_1 \neq x_2$ and $f_{\hat{k}}(0) = 0, \hat{k} = 1, 2, \cdots, n$. The master system is considered (1) and the corresponding slave system is described as given below:

$$\dot{m}(t) = -Mm(t) + Cf(m(t)) + \sum_{j=1}^{N} W_j f(m(t-\hat{\tau}_j(t))) + V(t) + u(t) + w(t), \tag{3}$$

where $u(t)$ and $w(t)$ represent the control input and the disturbance input which belongs to $\mathcal{L}_2[0, \infty)$ respectively. The error signal is taken as $r(t) = m(t) - v(t)$ in this paper. Thus, the synchronization error system can be described as follows:

$$\dot{r}(t) = -Mr(t) + Cg(r(t)) + \sum_{j=1}^{N} W_j g(r(t-\hat{\tau}_j(t))) + u(t) + w(t), \tag{4}$$

where $g(r(t)) = f(m(t)) - f(v(t))$. To completely utilize advanced computing technologies, the sampled-data control has been used to synchronize delayed RNNs. The following sampled-data controller is used here.

$$u(t) = \bar{K}r(t_k), \quad t \in [t_k, t_{k+1}).$$

Now, we consider the following non-fragile sampled-data controller

$$u(t) = (\bar{K} + \Delta\bar{K}(t))r(t_k). \tag{5}$$

Here, $\bar{K}$ refers to the gain matrix of sampled-data controller and the real-valued matrix $\Delta\bar{K}(t)$ represents the possible controller gain fluctuation. Assume that the sampling intervals satisfy $0 < t_{k+1} - t_k = h_k \leq h$, where $h(t) = t - t_k$ for $t \in [t_k, t_{k+1})$ and $h > 0$ denotes the largest sampling interval. $r(t_k)$ is discrete measurement of $r(t)$ at the sampling instant t_k.

Substituting (5) in (4), we have

$$\begin{aligned}\dot{r}(t) = -Mr(t) + Cg(r(t)) + \sum_{j=1}^{N} W_j g(r(t - \hat{\tau}_j(t)))\\ +(\bar{K} + \Delta\bar{K}(t))r(t_k) + w(t).\end{aligned} \tag{6}$$

Furthermore, the output error system of (6) is defined as follows:

$$y(t) = r(t) + \sum_{j=1}^{N} r(t - \hat{\tau}_j(t)). \tag{7}$$

The following are the Assumptions that have been used.

A1: We assume the time-varying delays to be bounded as shown below.

$$0 \leq \hat{\tau}_j(t) \leq \hat{\tau}_j, \tag{8}$$

and $\dot{\hat{\tau}}_j(t) \leq \eta_j$, where $\hat{\tau}_j$, η_j refer to positive constants.

A2: The conditions described below are satisfied by the neuron activation functions $g_{\hat{k}}(\cdot)$.

$$s_{\hat{k}}^{-} \leq \frac{g_{\hat{k}}(r_{\hat{k}})}{r_{\hat{k}}} \leq s_{\hat{k}}^{+}, \tag{9}$$

for all $r_{\hat{k}} \neq 0$ and $g_{\hat{k}}(0) = 0$, $\hat{k} = 1, 2, \cdots, n$.

A3: Matrices χ_1, χ_2, χ_3 and χ_4 satisfy the following conditions:

1. $\chi_1 = \chi_1^T \leq 0$, $\chi_3 = \chi_3^T > 0$, $\chi_4 = \chi_4^T \geq 0$,
2. $(||\chi_1|| + ||\chi_2||) . ||\chi_4|| = 0$.

The Definitions and Lemmas required in further derivation of the results are given below.

Definition 1 [29]: For given matrices χ_1, χ_2, χ_3 and χ_4 satisfying Assumption (A3), the neural network (6) with (7) is known as extended dissipative, if there exists a scalar $\delta > 0$ such that, for all $t_f \geq 0$, the subsequent inequality holds.

$$\int_0^{t_f} J(t)dt \geq \sup \; y^T(t)\chi_4 y(t) + \delta, 0 \leq t \leq t_f, \tag{10}$$

where $J(t) = y^T(t)\chi_1 y(t) + 2y^T(t)\chi_2 w(t) + w^T(t)\chi_3 w(t)$.

Definition 2 [29]: Suppose that $w(t) = 0$. Then, the system (6) is quadratically stable, if there exists a scalar $\nu > 0$ such that the derivative of the Lyapunov function in terms of time t satisfies $\dot{V}(r(t)) \leq -\nu|r(t)|^2$.

Lemma 1 [4]: For any matrix $W > 0$, scalars a and b satisfying $b > a$, a vector function $\omega : [a, b] \in \mathbb{R}^n$ such that the integrations are well-defined, we have

$$\begin{aligned}(b-a)\int_a^b \omega^T(\alpha)W\omega(\alpha)d\alpha\\ \geq \left[\int_a^b \omega(\alpha)d\alpha\right]^T W \left[\int_a^b \omega(\alpha)d\alpha\right].\end{aligned} \tag{11}$$

Lemma 2 [5]: For a given symmetric positive matrix $R \in \mathbb{R}^n$, any differentiable function r in $[a, b] \rightarrow \mathbb{R}^n$, then the subsequent inequality holds:

$$\int_a^b \dot{r}^T(u)R\dot{r}(u)du \geq \frac{1}{b-a}\phi^T \operatorname{diag}\{R, 3R, 5R\}\phi, \tag{12}$$

where

$$\phi = \begin{bmatrix} r(b) - r(a) \\ r(b) + r(a) - \frac{2}{b-a}\int_a^b r(u)du \\ r(b) - r(a) - \frac{6}{b-a}\int_a^b \delta_{a,b}(u)r(u)du \end{bmatrix}, \tag{13}$$

where $\delta_{a,b}(u) = 2\left(\frac{u-a}{b-a}\right) - 1$.

Lemma 3 [7]: For a differentiable function $r : [\alpha, \beta] \rightarrow \mathbb{R}^n$, a positive integer $k \in \mathbb{N}$, $m \in \mathbb{Z}_{\geq 0}$, a positive definite matrix $R \in \mathbb{R}^{n\times n}$, vector $\xi \in \mathbb{R}^{kn}$, and any matrices $N_i \in \mathbb{R}^{kn\times n}(i = 1, \cdots, m+1)$, the following inequality holds:

$$\begin{aligned}-\int_\alpha^\beta \dot{r}^T(s)R\dot{r}(s)ds \leq \sum_{i=1}^{m+1} \frac{\beta-\alpha}{2i-1}\xi^T N_i R^{-1} N_i\\ +Sym(N_i\psi_{i-1}(\alpha, \beta))\xi,\end{aligned} \tag{14}$$

where

$$\psi_i(\alpha, \beta) = \begin{cases} r(\beta) - r(\alpha), i = 0; \\ r(\beta) - (-1)^i r(\alpha) - \sum_{j=1}^{i} l_j^i \frac{j!}{(\beta-\alpha)^j}\rho_{(j-1)} \\ (\alpha, \beta), i \in \mathbb{N}^*, \end{cases}$$

$$\rho_m(\alpha, \beta) = \int_{s_o}^{\beta}\int_{s_1}^{\beta}\cdots\int_{s_m}^{\beta} r(s_{m+1})ds_{m+1}\cdots ds_1, \quad s_o = \alpha;$$

$$l_j^i = (-1)^{j+i}\binom{i}{j}\binom{i+j}{j}.$$

Lemma 4 [15]: Let A, B, P be matrices satisfying $P > 0$. Then, $\begin{pmatrix} B & A^T \\ A & -P \end{pmatrix} < 0$ iff $B + A^T P^{-1} A < 0$.

Lemma 5 [15]: Let Y, Q and $\Delta(t)$ be real matrices with appropriate dimensions. In addition, $\Delta(t)$ satisfies $\Delta^T(t)\Delta(t) \leq I$. Then, for any constant $\epsilon > 0$, the subsequent inequality holds:

$$Y\Delta(t)Q + Q^T\Delta^T(t)Y^T \leq \epsilon YY^T + \epsilon^{-1}Q^TQ.$$

This Remark 1 is derived from Lemma 3 when $m = 1$.

Remark 1: *For a differentiable function $r : [\alpha, \beta] \to \mathbb{R}^n$, a positive integer $k \in \mathbb{N}$, a positive definite matrix $R \in \mathbb{R}^{n\times n}$, any vector $\xi \in \mathbb{R}^{kn}$, and any matrices $N_i \in \mathbb{R}^{kn\times n}(i = p, q)$, the following inequality holds*:

$$-\int_\alpha^\beta \dot{r}^T(s)R\dot{r}(s)ds \le \xi^T[(\beta-\alpha)(N_pR^{-1}N_p^T + \frac{1}{3}N_qR^{-1}N_q^T) + Sym(N_pE_1 + N_qE_2)]\xi, \tag{15}$$

where $E_1\xi = r(\beta) - r(\alpha), E_2\xi = r(\beta) + r(\alpha) - \frac{2}{\beta-\alpha}\int_\alpha^\beta r(s)ds.$

Remark 2: *We can assign values to the weighting matrices so that the concept of extended dissipativity gives a general solution.*

(1) $\mathcal{L}_2 - \mathcal{L}_\infty$ *performance:* $\chi_1 = 0,\ \chi_2 = 0,\ \chi_3 = \tilde{\gamma}^2 I,\ \chi_4 = I$, *and* $\delta = 0$

(2) H_∞ *performance:* $\chi_1 = -I,\ \chi_2 = 0,\ \chi_3 = \tilde{\gamma}^2 I,\ \chi_4 = 0$, *and* $\delta = 0$

(3) Passivity performance: $\chi_1 = 0,\ \chi_2 = I,\ \chi_3 = \tilde{\gamma},\ \chi_4 = 0$, *and* $\delta = 0$

(4) Mixed H_∞ *and Passivity performance:* $\chi_1 = \tilde{\gamma}^{-1}\alpha I,\ \chi_2 = (1 = \alpha)I,\ \chi_3 = \tilde{\gamma}I,\ \chi_4 = 0$ *and* $\alpha = 0.4$

(5) $(\mathcal{Q} - \mathcal{S} - \mathcal{R})$ *Dissipativity:* $\chi_1 = \mathcal{Q},\ \chi_2 = \mathcal{S},\ \chi_3 = \mathcal{R} - \tilde{\alpha}I$, *and* $\chi_4 = 0$

III. MAIN RESULTS

In the following Theorems, we design the non-fragile sampled-data control and some sufficient conditions are given to guarantee that the error system (6) and (7) is synchronizes and extended dissipative in the form of LMIs. First, we assume that in Theorem 1 ($\Delta\bar{K}(t) = 0$).

Theorem 1: *Assume that (A1) and (A2) hold. For given scalars* $0 < \beta < 1, h > 0, \tilde{\tau}_j > 0, \eta_j > 0, \epsilon_1 > 0, \epsilon_2 > 0$, *matrices* $\chi_l,\ l = 1, 2, 3, 4$ *satisfying (A3), the error system (6) and (7) achieves quadratically stable and extended dissipative synchronization, if there exist symmetric matrices* $D = diag(d_1, d_2, \cdots, d_n) > 0, H_j > 0, L_j > 0, B_j > 0, \bar{X} \in R^{3n\times 3n} > 0, \bar{R} > 0, R > 0, P > 0, \bar{U} = \begin{bmatrix} \bar{U}_1 & \bar{U}_2 \\ * & \bar{U}_4 \end{bmatrix} > 0,\ Y > 0, A > 0, G > 0$, *any matrices* $N_{pj} > 0, N_{qj} > 0, M_{pj} > 0, M_{qj} > 0,\ (j = 1, \cdots, N)$ *and positive diagonal matrices* $F, F_1, \cdots, F_N$, *such that the following LMIs (16), as shown at the bottom of the next page hold with* $h(t) = \{0, h\}$:

$$\pi = \begin{bmatrix} \pi_{11} & \pi_{12} \\ \star & \pi_{22} \end{bmatrix} > 0,$$

$$\Xi = \sum_{m=1}^{8} \Xi_m,$$

where

$$\begin{aligned}
\Xi_1 &= -2e_1Pe_{2N+7}^T + 2e_{N+2}De_{2N+7}^T + e_{N+2}\sum_{j=1}^{N} L_je_{N+2}^T \\
&\quad -(1-\eta_1)e_{N+3}L_1e_{N+3}^T - \cdots - (1-\eta_N)e_{2N+2}L_N \\
&\quad \times e_{2N+2}^T + e_1\sum_{j=1}^{N} H_je_1^T - (1-\eta_1)e_2H_1e_2^T - \cdots \\
&\quad -(1-\eta_N)e_{N+1}H_Ne_{N+1}^T + \sum_{j=1}^{N} e_{2N+7}(\hat{\tau}_jB_j)e_{2N+7}^T \\
&\quad + \sum_{j=1}^{N} \text{sym}\left(N_{pj}E_1^j + N_{qj}E_2^j\right) \\
&\quad + \sum_{j=1}^{N} \text{sym}(M_{pj}E_3^j + M_{qj}E_4^j),
\end{aligned}$$

$$\begin{aligned}
\Xi_2 &= -[e_{2N+3}\ \ e_{2N+8}\ \ e_1 - e_{2N+3}]\bar{X}[e_{2N+3}\ \ e_{2N+8} \\
&\quad e_1 - e_{2N+3}]^T + [e_1\ \ e_{2N+7}\ \ 0]\bar{X}[e_1\ \ e_{2N+7}\ \ 0]^T \\
&\quad +2[he_{2N+5}\ \ e_1 - e_{2N+3}\ \ h(e_1 - e_{2N+5})]\bar{X} \\
&\quad [0\ \ 0\ \ e_{2N+7}]^T,
\end{aligned}$$

$$\Xi_3 = e_{2N+4}(h - h(t))\bar{R}e_{2N+4}^T - e_{2N+4}h(t)\bar{R}e_{2N+4}^T,$$

$$\begin{aligned}
\Xi_4 &= -2e_{2N+4}\bar{U}_2(e_1 - e_{2N+4})^T + [e_{2N+7}\ e_{2N+7}] \\
&\quad \times(h - h(t))\begin{bmatrix} \bar{U}_1 & \bar{U}_2 \\ \star & \bar{U}_4 \end{bmatrix}[e_{2N+7}\ \ e_{2N+4}]^T \\
&\quad -h(t)e_{2N+4}\bar{U}_3e_{2N+4}^T - \text{sym}(Y^TA),
\end{aligned}$$

$$\Xi_5 = h^2e_{2N+7}Re_{2N+7}^T - \phi^T\text{diag}\{R, 3R, 5R\}\phi,$$

$$\begin{aligned}
\Xi_6 &= -e_1\epsilon_1Ge_{2N+7}^T - e_1\epsilon_1(GM + M^TG^T)e_1^T \\
&\quad +e_1\epsilon_1GCe_{N+2}^T + e_1\left(\epsilon_1GW_1\right)e_{N+3}^T \\
&\quad +\cdots + e_1\left(\epsilon_1GW_N\right)e_{2N+2}^T \\
&\quad +e_1\epsilon_1Le_{2N+4}^T - e_{2N+7}\epsilon_2(G + G^T)e_{2N+7}^T \\
&\quad -e_{2N+7}\epsilon_2M^TG^Te_1^T + e_{2N+7}\epsilon_2C^TG^Te_{N+2}^T \\
&\quad +e_{2N+7}\left(\epsilon_2W_1^TG^T\right)e_{N+3}^T + \cdots \\
&\quad +e_{2N+7}\left(\epsilon_2W_N^TG^T\right)e_{2N+2}^T + e_{2N+7}\epsilon_2L^Te_{2N+4}^T,
\end{aligned}$$

$$\begin{aligned}
\Xi_7 &= -2[\kappa_1e_1 - e_{N+2}]F[e_{N+2} - \kappa_2e_1]^T \\
&\quad -2[\kappa_1e_2 - e_{N+3}]F_1[e_{N+3} - \kappa_2e_2]^T - \cdots \\
&\quad -2[\kappa_1e_{N+1} - e_{2N+2}]F_N[e_{2N+2} - \kappa_2e_{N+1}]^T,
\end{aligned}$$

$$\begin{aligned}
\Xi_8 &= [e_1\ \ e_{2N+2}]\chi_1[e_1\ \ e_{2N+2}]^T + 2[e_1\ \ e_{2N+2}]\chi_2\ e_{4N+10}^T \\
&\quad +e_{4N+10}\chi_3\ e_{4N+10}^T,
\end{aligned}$$

$$\pi_{11} = \beta P - \chi_4, \pi_{12} = [\pi_{12}^1, \cdots, \pi_{12}^N], \pi_{12}^l = -\chi_4,$$

$$\pi_{12} = [\pi_{22}^1, \cdots, \pi_{22}^N], \pi_{22}^l = (1-\beta)P - \chi_4,\ l = 1, \cdots, N.$$

Here, $e_i = [0_{n\times(i-1)n}\ \ \ I_n\ \ \ 0_{n\times(4N+10-i)n}]^T,\ i = 1, 2, \cdots, 4N+10,$
$\phi^T = [e_1 - e_{2N+3}\ \ e_1 + e_{2N+3} - 2e_{2N+5}\ \ e_1 - e_{2N+3} - 6e_{2N+6}],\ \ \underline{\hat{\tau}}_j = \tilde{\tau}_j - \hat{\tau}_j(t), \kappa_1 = diag(s_1^-, s_2^-, \cdots, s_n^-), \kappa_2 = diag(s_1^+, s_2^+, \cdots, s_n^+).$

Moreover, if the LMIs (16) is solvable, the desired controller gain matrix is given by $\bar{K} = G^{-1}L$.

Proof: Consider the LKF as given below:

$$V(r(t)) = \sum_{l=1}^{5} V_l(r(t)), \qquad t \in [t_k, t_{k+1}), \tag{17}$$

where

$$V_1(r(t)) = r^T(t)Pr(t) + 2\sum_{\hat{k}=1}^{n} d_{\hat{k}} \int_0^{r_{\hat{k}}(t)} g_j(s)ds + \sum_{j=1}^{N}\int_{t-\hat{\tau}_j(t)}^{t}\Big[g^T(r(s))L_j g(r(s))ds + r^T(s)H_j r(s)ds\Big] + \sum_{j=1}^{N}\int_{-\hat{\tau}_j}^{0}\int_{t+\theta}^{t}\dot{r}^T(s)B_j\dot{r}(s)dsd\theta,$$

$$V_2(r(t)) = \int_{t-h}^{t}\eta_1^T(s)\bar{X}\eta_1(s)ds,$$

$$V_3(r(t)) = (t_{k+1}-t)(t-t_k)r^T(t_k)\bar{R}r(t_k),$$

$$V_4(r(t)) = (h-(t-t_k))\int_{t_k}^{t}\eta_2^T(s)\bar{U}\eta_2(s)ds,$$

$$V_5(r(t)) = h\int_{-h}^{0}\int_{t+\alpha}^{t}\dot{r}^T(s)R\dot{r}(s)dsd\alpha,$$

with $\eta_1(s) = \Big[r^T(s), \dot{r}^T(s), \int_s^t \dot{r}^T(v)dv\Big]^T$, $\eta_2(s) = \big[\dot{r}^T(s), r^T(t_k)\big]^T$.

The time-derivative of $V_l(r(t))$ $(l = 1, 2, \cdots, 5)$ are given by

$$\dot{V}_1(r(t)) \leq -2r^T(t)P\dot{r}(t) + 2g^T(r(t))D\dot{r}(t) + \sum_{j=1}^{N}\Big[g^T(r(t))L_j g(r(t)) - (1-\eta_j)g^T(r(t-\hat{\tau}_j(t)))L_j g(r(t-\hat{\tau}_j(t)))\Big] + \sum_{j=1}^{N}\Big[r^T(t)H_j r(t) - (1-\eta_j)r^T(t-\hat{\tau}_j(t)) \times H_j r(t-\hat{\tau}_j(t))\Big] + \sum_{j=1}^{N}\hat{\tau}_j\dot{r}^T(t)B_j\dot{r}(t) - \sum_{j=1}^{N}\int_{t-\hat{\tau}_j}^{t}\dot{r}^T(s)B_j\dot{r}(s)ds.$$

Using Remark 1, the last integral term in the above inequality becomes

$$-\sum_{j=1}^{N}\int_{t-\hat{\tau}_j}^{t}\dot{r}^T(s)B_j\dot{r}(s)ds = \sum_{j=1}^{N}\Big[-\int_{t-\hat{\tau}_j}^{t-\hat{\tau}_j(t)}\dot{r}^T(s) \times B_j\dot{r}(s)ds - \int_{t-\hat{\tau}_j(t)}^{t}\dot{r}^T(s)B_j\dot{r}(s)ds\Big]$$
$$\leq \xi^T(t)\Big[\sum_{j=1}^{N}\underline{\hat{\tau}}_j\Big(N_{pj}B_j^{-1}N_{pj}^T + \frac{1}{3}N_{qj}B_j^{-1}N_{qj}^T\Big) + \text{sym}(N_{pj}E_1^j + N_{qj}E_2^j) + \sum_{j=1}^{N}\hat{\tau}_j(t)\Big(M_{pj}B_j^{-1}M_{pj}^T + \frac{1}{3}M_{qj}B_j^{-1}M_{qj}^T\Big) + \text{sym}(M_{pj}E_3^j + M_{qj}E_4^j)\Big]\xi(t),$$

where

$$E_1^j\xi = r(t-\hat{\tau}_j(t)) - r(t-\hat{\tau}_j)),$$

$$E_2^j\xi = r(t-\hat{\tau}_j(t)) + r(t-\hat{\tau}_j)) - \frac{2}{\hat{\tau}_j - \hat{\tau}_j(t)}\int_{t-\hat{\tau}_j}^{t-\hat{\tau}_j(t)} r(s)ds,$$

$E_3^j\xi = r(t) - r(t-\hat{\tau}_j(t))$, and

$$E_4^j\xi = r(t) + r(t-\hat{\tau}_j(t)) - \frac{2}{\hat{\tau}_j(t)}\int_{t-\hat{\tau}_j(t)}^{t} r(s)ds,$$

for $j = 1, 2, \cdots, N$. Then, we get

$$\dot{V}_1(r(t)) \leq \xi^T(t)\Big(\Xi_1 + \sum_{j=1}^{N}\underline{\hat{\tau}}_j\Big(N_{pj}B_j^{-1}N_{pj}^T + \frac{1}{3}N_{qj}B_j^{-1}N_{qj}^T\Big)$$

$$\Psi = \begin{pmatrix} \Xi & \sum_{j=1}^{N}\underline{\hat{\tau}}_j N_{pj} & \sum_{j=1}^{N}\frac{\underline{\hat{\tau}}_j}{3}N_{qj} & \sum_{j=1}^{N}\hat{\tau}_j M_{pj} & \sum_{j=1}^{N}\frac{\hat{\tau}_j}{3}M_{qj} & h(t)Y^T \\ \star & -\sum_{j=1}^{N}\underline{\hat{\tau}}_j B_j & 0 & 0 & 0 & 0 \\ \star & \star & -\sum_{j=1}^{N}\frac{\underline{\hat{\tau}}_j}{3}B_j & 0 & 0 & 0 \\ \star & \star & \star & -\sum_{j=1}^{N}\hat{\tau}_j B_j & 0 & 0 \\ \star & \star & \star & \star & -\sum_{j=1}^{N}\frac{\hat{\tau}_j}{3}B_j & 0 \\ \star & \star & \star & \star & \star & -h(t)\bar{U}_1 \end{pmatrix} < 0, \tag{16}$$

$$+\sum_{j=1}^{N}\hat{\tau}_j(t)\Big(M_{pj}B_j^{-1}M_{pj}^T + \frac{1}{3}M_{qj}B_j^{-1}M_{qj}^T\Big)\Big)\xi(t), \tag{18}$$

$$\dot{V}_2(r(t)) = -\begin{bmatrix} r(t-h) \\ \dot{r}(t-h) \\ r(t)-r(t-h)\end{bmatrix}^T \bar{X}\begin{bmatrix} r(t-h) \\ \dot{r}(t-h) \\ r(t)-r(t-h)\end{bmatrix} + \begin{bmatrix} r(t) \\ \dot{r}(t) \\ 0\end{bmatrix}^T \bar{X}\begin{bmatrix} r(t) \\ \dot{r}(t) \\ 0\end{bmatrix} + 2\begin{bmatrix} \int_{t-h}^{t} r(s)ds \\ r(t)-r(t-h) \\ hr(t)-\int_{t-h}^{t} r(s)ds\end{bmatrix}^T \bar{X}\begin{bmatrix} 0 \\ 0 \\ \dot{r}(t)\end{bmatrix},$$
$$= \xi^T(t)\Xi_2\xi(t), \tag{19}$$

$$\begin{aligned}\dot{V}_3(r(t)) &= (t_{k+1}-t)r^T(t_k)\bar{R}r(t_k) - (t-t_k)r^T(t_k)\bar{R}r(t_k),\\ &\leq (h-(t-t_k))r^T(t_k)\bar{R}r(t_k)\\ &\quad -(t-t_k)r^T(t_k)\bar{R}r(t_k),\\ &= \xi^T(t)\Xi_3\xi(t),\end{aligned} \tag{20}$$

$$\begin{aligned}\dot{V}_4(r(t)) &= -2r^T(t_k)\bar{U}_2\left[r(t)-r(t_k)\right] - (t-t_k)r^T(t_k)\\ &\quad \bar{U}_3 r(t_k) + (h-(t-t_k))\eta_2^T(t)\bar{U}\eta_2(t)\\ &\quad -\int_{t_k}^{t}\dot{r}^T(s)\bar{U}_1\dot{r}(s)ds.\end{aligned}$$

Using Lemma 1, we obtain

$$-\int_{t_k}^{t}\dot{r}^T(s)\bar{U}_1\dot{r}(s)ds \leq -\frac{1}{t-t_k}\xi^T(t)A^T\bar{U}_1A\xi(t).$$

For any matrix Y, it is quite simple to obtain

$$\frac{1}{t-t_k}\left(\bar{U}_1A-(t-t_k)Y\right)^T\bar{U}_1^{-1}\left(\bar{U}_1A-(t-t_k)Y\right) \geq 0.$$

Thus, we see that the following inequality is true.

$$-\frac{1}{t-t_k}\left[A^T\bar{U}_1A\right] \leq -sym(Y^TA) + (t-t_k)Y^T\bar{U}_1^{-1}Y,$$

where $A = [e_1 - e_{2N+4}]$. Therefore,

$$\dot{V}_4(r(t)) \leq \xi^T(t)\left(\Xi_4 + (t-t_k)Y^T\bar{U}_1^{-1}Y\right)\xi(t), \tag{21}$$

$$\dot{V}_5(t) = h^2\dot{r}^T(t)R\dot{r}(t) - h\int_{t-h}^{t}\dot{r}^T(s)R\dot{r}(s)ds. \tag{22}$$

Using the Lemma 2, we get

$$-h\int_{t-h}^{t}\dot{r}^T(s)R\dot{r}(s)\ ds \leq -\xi^T(t)\left(\phi^T diag\{R, 3R, 5R\}\phi\right)\xi(t),$$

where

$$\phi^T = [e_1 - e_{2N+3}, e_1 + e_{2N+3} - 2e_{2N+5}, e_1 - e_{2N+3} - 6e_{2N+6}].$$

It follows from (22), we get

$$\begin{aligned}\dot{V}_5(r(t)) &\leq \xi^T(t)(h^2\dot{r}^T(t)R\dot{r}(t)\\ &\quad +\phi^T diag\{R, 3R, 5R\}\phi)\xi(t),\\ \dot{V}_5(r(t)) &\leq \xi^T(t)\Xi_5\xi(t).\end{aligned} \tag{23}$$

Given the error system (4), and any matrix G with suitable dimensions and scalars $\epsilon_1 > 0$, $\epsilon_2 > 0$, it is possible to have that

$$\begin{aligned}0 &= 2\left(\epsilon_1 r^T(t) + \epsilon_2\dot{r}^T(t)\right)\times G\Big[-\dot{r}(t) - Mr(t) + Cg(r(t))\\ &\quad + \sum_{j=1}^{N}W_jg(r(t-\hat{\tau}_j(t))) + \bar{K}r(t_k)\Big]\\ &= \xi^T(t)\Xi_6\xi(t).\end{aligned} \tag{24}$$

From (9), we can say that there exist diagonal matrices $F \geq 0$ and $F_j \geq 0$, $(j = 1, \cdots, N)$ such that the subsequent inequalities are satisfied:

$$\begin{aligned}&2\left[\kappa_1 r(t) - g(r(t))\right]^T F\left[g(r(t)) - \kappa_2 r(t)\right] \geq 0,\\ &2\sum_{j=1}^{N}\left[\kappa_1 r(t-\hat{\tau}_j(t)) - g(r(t-\hat{\tau}_j(t)))\right]^T F_j\\ &\quad\left[g(r(t-\hat{\tau}_j(t))) - \kappa_2 r(t-\hat{\tau}_j(t))\right] \geq 0.\end{aligned} \tag{25}$$

From the above inequalities (25), we have

$$\xi^T(t)\Xi_7\xi(t) \geq 0. \tag{26}$$

Now, combining (18)-(26) with $L = G\bar{K}$ and then using Lemma 4 yields,

$$\begin{aligned}\dot{V}(r(t)) - J(t) &< \xi^T(t)\Big[\sum_{m=1}^{7}\Xi_m + \sum_{j=1}^{N}\underline{\tau}_j\Big(N_{pj}B_j^{-1}N_{pj}^T\\ &\quad + \frac{1}{3}N_{qj}B_j^{-1}N_{qj}^T\Big) + \sum_{j=1}^{N}\hat{\tau}_j(t)\Big(M_{pj}B_j^{-1}M_{pj}^T\\ &\quad + \frac{1}{3}M_{qj}B_j^{-1}M_{qj}^T\Big)\\ &\quad + (t-t_k)Y^T\bar{U}_1^{-1}Y\Big]\xi(t),\\ &< \xi^T(t)\Psi\xi(t),\\ \dot{V}(r(t)) &< 0,\end{aligned} \tag{27}$$

where

$$\begin{aligned}\xi(t) = [&r^T(t), r^T(t-\hat{\tau}_1(t)), \cdots, r^T(t-\hat{\tau}_N(t)), g^T(r(t)),\\ &g^T(r(t-\hat{\tau}_1(t))), \cdots, g^T(r(t-\hat{\tau}_N(t))), r^T(t-h), r^T(t_k),\\ &\int_{t-h}^{t}\frac{r^T(s)}{h}ds, \frac{1}{h}\int_{t-h}^{t}\delta_{t-h,t}(s)r^T(s)ds, \dot{r}^T(t), \dot{r}^T(t-h),\\ &r^T(t-\hat{\tau}), \underline{l}^1, \cdots, \underline{l}^N, \bar{l}^1, \cdots, \bar{l}^N, w^T(t)]^T,\end{aligned}$$

$$\delta_{t-h,t}(s) = 2\left(\frac{s-t+h}{h}\right) - 1,$$

$$\underline{l}^j = \frac{1}{\hat{\tau} - \hat{\tau}_j(t)}\int_{t-\hat{\tau}}^{t-\hat{\tau}_j(t)} r^T(s)ds$$

and $\bar{l}^j = \frac{1}{\hat{\tau}_j(t)}\int_{t-\hat{\tau}_j(t)}^{t} r^T(s)ds$ for $j = 1, 2, \cdots, N$.

Since $\Psi < 0$, there exists a small scalar $\nu > 0$, such that $\Psi < -\nu I$, then

$$\dot{V}(r(t)) - J(t) \leq -\nu|\xi(t)|^2 \leq -\nu|r(t)|^2, \quad i.e., \dot{V}(r(t)) \leq J(t) - \nu|r(t)|^2.$$

Considering $w(t) = 0$ yields

$$J(t) = y^T(t)\chi_1 y(t).$$

Noticing that $\chi_1 \leq 0$ under Assumption (A3) yields that $\dot{V}(r(t)) \leq -\nu|r(t)|^2$. From this, it can be inferred that the system (4) is quadratically stable.

Now, we consider the extended dissipativity condition for the system. It can be seen that,

$$\dot{V}(r(t)) - J(t) \leq \xi^T(t)[\Psi + \Xi_8]\xi(t), \quad \dot{V}(r(t)) - J(t) \leq 0. \tag{28}$$

Now, integrating (28) on both sides from 0 to t, we have

$$\int_0^t J(s)ds \geq V(r(t)) - V(r(0)) \geq r^T(t)Pr(t) + \delta, \tag{29}$$

where δ is chosen as $\delta = -V(r(0)) - \|P\| \sup_{-\hat{\tau}_j \leq s \leq 0} |\Gamma(s)|^2$.

The following two cases are essential to show that inequality (10) is valid. Therefore, we consider two cases as $\|\chi_4\| = 0$ and $\|\chi_4\| \neq 0$.

To begin with, if $\|\chi_4\| = 0$, then for any $t_f \geq 0$ (29) implies that,

$$\int_0^{t_f} J(t)dt \geq r^T(t_f)Pr(t_f) + \delta \geq \delta. \tag{30}$$

From this, it is evident that Theorem 1 holds well. If we consider $\|\chi_4\| \neq 0$, as written in Assumption (A3), it can be concluded that $\chi_1 = 0$, $\chi_2 = 0$ and $\chi_3 > 0$.
If $t_f \geq t \geq 0$, then we get

$$\int_0^{t_f} J(t)dt \geq \int_0^t J(s)ds \geq r^T(t)Pr(t) + \delta. \tag{31}$$

When $t > \hat{\tau}_j(t)$, we get $0 < t - \hat{\tau}_j(t) \leq t_f$.
Thus,

$$\int_0^{t_f} J(t)dt \geq \sum_{j=1}^{N}[r^T(t - \hat{\tau}_j(t))Pr(t - \hat{\tau}_j(t))] + \delta. \tag{32}$$

Furthermore, if $t \leq \hat{\tau}_j(t)$, we get $-\hat{\tau}_j \leq t - \hat{\tau}_j(t) \leq 0$, it could be verified that

$$\begin{aligned}
&\delta + \sum_{j=1}^{N}[r^T(t - \hat{\tau}_j(t))Pr(t - \hat{\tau}_j(t))] \\
&\leq \delta + \sum_{j=1}^{N} \|P\||r(t - \hat{\tau}_j(t))|^2 \\
&\leq \delta + \sum_{j=1}^{N} \|P\| \sup_{-\tau_j \leq \theta \leq 0} |\Gamma(\theta)|^2 \\
&= -V(r(0)) \leq \int_0^{t_f} J(t)dt.
\end{aligned}$$

It is clear from the above that (32) holds for any $t_f \geq t \geq 0$. From (31) and (32), we can say that there is a scalar $0 < \beta < 1$ satisfying

$$\int_0^{t_f} J(t)dt \geq \delta + \beta r^T(t)Pr(t) + (1 - \beta) \times \sum_{j=1}^{N}[r^T(t - \hat{\tau}_j(t))Pr(t - \hat{\tau}_j(t))]. \tag{33}$$

Noticing the fact that

$$\begin{aligned}
&y^T(t)\chi_4 y(t) \\
&= -\sum_{j=1}^{N}\begin{bmatrix} r(t) \\ r(t - \hat{\tau}_j(t)) \end{bmatrix}^T \pi \begin{bmatrix} r(t) \\ r(t - \hat{\tau}_j(t)) \end{bmatrix} \\
&\quad + \beta r^T(t)Pr(t) + \sum_{j=1}^{N}(1 - \beta)r^T(t - \hat{\tau}_j(t))Pr(t - \hat{\tau}_j(t)),
\end{aligned}$$

for $\pi > 0$, then

$$y^T(t)\chi_4 y(t) \leq \beta r^T(t)Pr(t) + \sum_{j=1}^{N}(1 - \beta)r^T(t - \hat{\tau}_j(t))Pr(t - \hat{\tau}_j(t)).$$

This shows that, for any $t \geq 0$, $t_f \geq 0$, with $t_f \geq t$,

$$\int_0^{t_f} J(t)dt \geq y^T(t)\chi_4 y(t) + \delta.$$

Thus, (10) holds for any $t_f \geq 0$. According to the above analysis, for $\|\chi_4\| = 0$ and $\|\chi_4\| \neq 0$, the error system considered in (6) is extended dissipative. □

Theorem 2: Assume that (A1) and (A2) hold. For given scalars $h > 0, \eta_j > 0, \hat{\tau}_j > 0, \epsilon > 0, \beta > 0, \epsilon_1 > 0, \epsilon_2 > 0$, *matrices* $\chi_l, l = 1, 2, 3, 4$ *satisfying (A3), the error system (6) and (7) achieves quadratically stable and extended dissipative, if there exist symmetric matrices* $D = diag(d_1, d_2, \cdots, d_n) > 0, H_j > 0, L_j > 0, B_j > 0, \bar{X} \in R^{3n \times 3n} > 0, \bar{R} > 0, R > 0, M > 0, P > 0, \bar{U} = \begin{bmatrix} \bar{U}_1 & \bar{U}_2 \\ \star & \bar{U}_4 \end{bmatrix}$, $Y > 0, A > 0, G > 0$, *any matrices* $N_{pj} > 0, N_{qj} > 0, M_{pj} > 0, M_{qj} > 0$ $(j = 1, \cdots, N)$ *and positive diagonal matrices* $F, F_1, \cdots, F_N$ *such that the following LMIs hold with* $h(t) = \{0, h\}$:

$$\pi = \begin{bmatrix} \pi_{11} & \pi_{12} \\ \star & \pi_{22} \end{bmatrix} > 0,$$

$$\Upsilon_1 = [\overbrace{0 \cdots 0}^{2N+2} \bar{H}^T G^T \;\; 0 \;\; 0 \;\; 0 \;\; \bar{H}^T G^T \;\; \overbrace{0 \cdots 0}^{2N+3}]^T,$$

$$\Upsilon_2 = [\bar{E} \;\; \overbrace{0 \cdots 0}^{2N+5} \;\; \bar{E} \;\; \overbrace{0 \cdots 0}^{2N+3}],$$

$$\begin{aligned}
\Xi_6 = &-e_1\epsilon_1 G e_{2N+7}^T - e_1\epsilon_1 G^T M e_1^T + e_1\epsilon_1 G C e_{N+2}^T + e_1 \\
&(\epsilon_1 G \sum_{j=1}^{N} W_j)(e_{N+3})^T + \cdots + e_1(\epsilon_1 G \sum_{j=1}^{N} W_j)e_{2N+2}^T \\
&-e_{2N+7}\epsilon_2 G e_{2N+7}^T - e_{2N+7}\epsilon_2 G M e_1^T
\end{aligned}$$

$$+e_{2N+7}\epsilon_2 G^T C e_{N+2}^T + e_{2N+7}(\epsilon_2 G^T \sum_{j=1}^{N} W_j)$$

$$e_{N+3}^T + \cdots + e_{2N+7}(\epsilon_2 G^T \sum_{j=1}^{N} W_j) e_{2N+2}^T,$$

and the other entries of Ψ are defined in the same way as in Theorem 1. Moreover, if the LMIs (34), as shown at the bottom of the page is non-fragile synchronized, the desired controller gain matrix is given by $\bar{K} = G^{-1}L$.

Proof: The non-fragile controller is considered as given below:

$$u(t) = (\bar{K} + \Delta\bar{K}(t))r(t_k). \tag{35}$$

Here, $\bar{K}$ denotes the controller gain matrix to be found. Here, $\Delta\bar{K}(t)$ which is a real-valued matrix, denotes the controller gain fluctuation. It can be assumed that $\Delta\bar{K}(t)$ takes the subsequent form:

$$\Delta\bar{K}(t) = \bar{H}\Delta(t)\bar{E}, \tag{36}$$

where $\Delta(t) \in \mathbb{R}^{k\times l}$ is the unknown time-varying matrix that satisfies $\Delta^T(t)\Delta(t) \leq I$. Here, $\bar{H}$ and $\bar{E}$ are considered as known matrices. Replace $\bar{K}$ by $\bar{K} + \Delta\bar{K}(t)$ in Theorem 1. As proceeded in the proof of Theorem 1, here the following can be obtained.

$$\Psi + \Upsilon_1\Delta\bar{K}(t)\Upsilon_2^T + \Upsilon_2\Delta\bar{K}^T(t)\Upsilon_1^T < 0. \tag{37}$$

By Lemma 5, (37) is equivalent to

$$\Psi + \epsilon^{-1}\Upsilon_1\Upsilon_1^T + \epsilon\Upsilon_2^T\Upsilon_2 < 0. \tag{38}$$

Applying Lemma 4, it follows that (38) is equivalent to (34). Hence, the theorem has been proved. □

Remark 3: Generally, synchronization designs with multiple time-varying delays, the extended dissipative case, non-fragile and sampled-data control are not simply applied to RNNs. Some research publications have tackled such problems [10], [15], [19], [20], [22], [31]. However, the authors used very simple LKFs to solve the stability problems in these articles. A new LKF with the information of multiple time-varying delays ($0 \leq \hat{\tau}_j(t) \leq \hat{\tau}_j$), augmented LKF approach, and utilizing Polynomial-Based Integral Inequality (PBII) technique have been proposed for the quadratically stable and extended dissipativie analysis in this paper. Having this in consideration, some less conservative results can occur in our method and it has been provided in the numerical example section. However, extended disspativity and non-fragile synchronization were completely studied for RNNs with multiple time-varying delays, which is the main contribution and motivation of our work.

Remark 4: Computational complexity will be a fundamental issue in line with larger LMI size and more decision variables. In our LMIs, the maximum number of decision variables are used in Theorems 1 and 2. Moreover, a larger LMIs size yields better performance. The newly introduced integral techniques are used in the construction of proper LKF to derive the results in Theorems, which produces tighter bounds than the existing one like the reciprocally convex approach, and so on. Maximum allowable bounds $\hat{\tau}_j$ and sampling period h are less conservative than the existing ones in the literature as seen in Table 1. In addition, the relaxations of the derived results are obtained at the cost of multiple decision variables. Having maximum allowable bounds $\hat{\tau}_j$ yields an efficient result, but to minimize the computational complexity burden, and time for computation, we will be using Finsler's Lemma in our future work to reduce the number of decision variables.

IV. SIMULATION RESULTS

In this part, we introduce simulation studies to demonstrate the adequacy of the control scheme proposed and the merits

$$\Omega = \begin{pmatrix} \Xi & \sum_{j=1}^{N}\hat{\tau}_j N_{pj} & \sum_{j=1}^{N}\frac{\hat{\tau}_j}{3}N_{qj} & \sum_{j=1}^{N}\hat{\tau}_j M_{pj} & \sum_{j=1}^{N}\frac{\hat{\tau}_j}{3}M_{qj} & h(t)Y^T & \Upsilon_1 & \epsilon\Upsilon_2^T \\ \star & -\sum_{j=1}^{N}\hat{\tau}_j B_j & 0 & 0 & 0 & 0 & 0 & 0 \\ \star & \star & -\sum_{j=1}^{N}\frac{\hat{\tau}_j}{3}B_j & 0 & 0 & 0 & 0 & 0 \\ \star & \star & \star & -\sum_{j=1}^{N}\hat{\tau}_j B_j & 0 & 0 & 0 & 0 \\ \star & \star & \star & \star & -\sum_{j=1}^{N}\frac{\hat{\tau}_j}{3}B_j & 0 & 0 & 0 \\ \star & \star & \star & \star & \star & -h(t)\bar{U}_1 & 0 & 0 \\ \star & \star & \star & \star & \star & \star & -\epsilon I & 0 \\ \star & \star & \star & \star & \star & \star & \star & -\epsilon I \end{pmatrix} < 0, \tag{34}$$

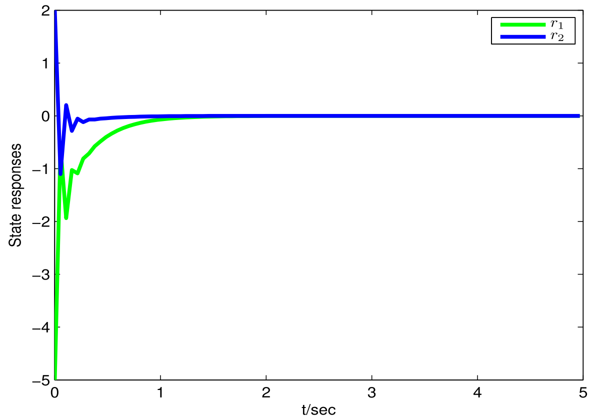

FIGURE 2. State trajectory of the system for $L_2 - L_\infty$ performance in Example 4.1.

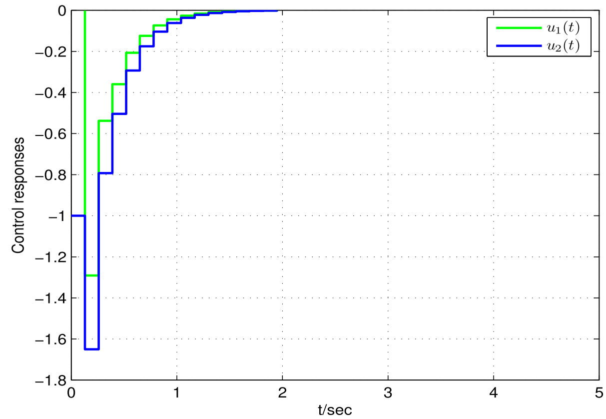

FIGURE 3. Control Response of the system $L_2 - L_\infty$ performance in Example 4.1.

of our methodology, in view of the conditions acquired in the previous section.

Example 1: Consider the RNNs with multiple time-varying delays as given below:

$$\dot{r}(t) = -Mr(t) + Cg(r(t)) + \sum_{j=1}^{2} W_j g(r(t - \hat{\tau}_j(t))) + u(t) + w(t), \quad (39)$$

where

$$M = \begin{bmatrix} 5 & 0 \\ 0 & 4 \end{bmatrix}, \; C = \begin{bmatrix} 1 & 0.4 \\ -2 & 0.1 \end{bmatrix},$$
$$W_1 = \begin{bmatrix} 0.5 & 0.7 \\ 0.7 & 0.4 \end{bmatrix}, \; W_2 = \begin{bmatrix} 0.3 & 0.2 \\ 0.1 & 0.6 \end{bmatrix}.$$

Here Assumption (A2) is satisfied with the values $s_1^- = -0.1,\ s_1^+ = 0.1,\ s_2^- = -0.2,\ s_2^+ = 0.2$. *Assume that* $h = 0.4$ *and the corresponding time-delays are taken as* $\hat{\tau}_1(t) = 0.3sin(t) + 0.2,\ \hat{\tau}_2(t) = 0.1sin(t) + 0.6,\ \hat{\tau}_1 = 0.5,\ \hat{\tau}_2 = 0.7,\ \beta = 0.4,\ \epsilon_1 = 1.5,\ \epsilon_2 = 0.5$. *Having these parameters in our consideration, MATLAB LMI toolbox is used to solve the LMIs in Theorem 2, and then we establish the subsequent parts of the extended dissipative conditions for the system (39). Moreover, the extended dissipative condition contains* $\mathcal{L}_2 - \mathcal{L}_\infty$ *performance, passivity,* H_∞ *performance, mixed passivity and* H_∞ *performance and also* $(\mathcal{Q} - \mathcal{S} - \mathcal{R})$*-dissipativity as special cases. The extended dissipative examination of system (39) is concentrated here on the weighting matrices* $\chi_1, \chi_2, \chi_3,$ *and* χ_4.

$\mathcal{L}_2 - \mathcal{L}_\infty$ *performance:* $\chi_1 = 0,\ \chi_2 = 0,\ \chi_3 = \tilde{\gamma}^2 I,\ \chi_4 = I$ *and* $\delta = 0$. *By using the above parameters, we are able to acquire the following control gain matrix* $\bar{K}$ *by figuring out the feasibility problem for the LMIs in Theorem 2 and MATLAB LMI toolbox.*

$$\bar{K} = \begin{bmatrix} 0.3435 & 0.0242 \\ 0.0213 & 0.0403 \end{bmatrix}.$$

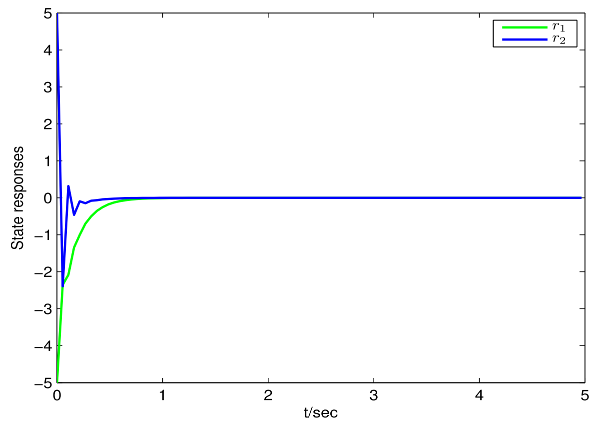

FIGURE 4. State trajectory of the system for H_∞ performance in Example 4.1.

The state trajectories and the control response of the system (39) under randomized initial conditions are seen in Fig. 2 and Fig. 3 respectively. It is noted from Figs. 2 and 3 that the system state and control inputs of the system are able to keep the system stable (converges to zero) and behaves $\mathcal{L}_2 - \mathcal{L}_\infty$ *performance under the above mentioned parameter values, which indicates that the designed controller is effective. Clearly, the simulation result demonstrates that the suggested approach is feasible and efficient.*

H_∞ *performance:* $\chi_1 = -I,\ \chi_2 = 0,\ \chi_3 = \tilde{\gamma}^2 I,\ \chi_4 = 0,$ *and* $\delta = 0$. *It can be easily estimated using the LMIs stated in Theorem 2, and the resulting control gain matrix is*

$$\bar{K} = \begin{bmatrix} 0.4211 & 0.0034 \\ 0.0352 & 0.0314 \end{bmatrix}.$$

At the same time, the relative simulation shown in Fig. 4 explains the subsequent evolution of the state response curves with respect to the control gain matrix. Fig. 5 shows the control response of the system (39). Thus, the system under consideration performs well.

Passivity performance: $\chi_1 = 0,\ \chi_2 = I,\ \chi_3 = \tilde{\gamma},\ \chi_4 = 0,$ *and* $\delta = 0$. *Now, the unified system examination turns to*

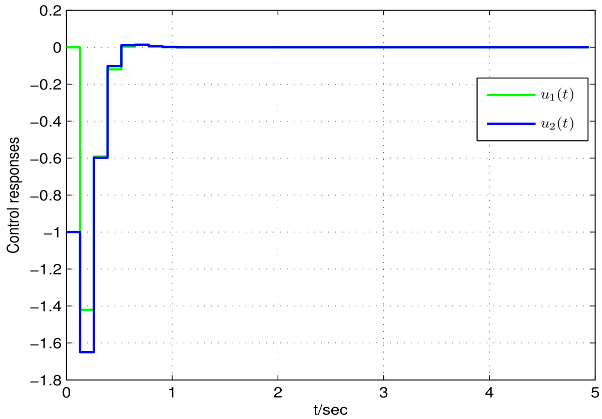

FIGURE 5. Control Response of the system for H_∞ performance in Example 4.1.

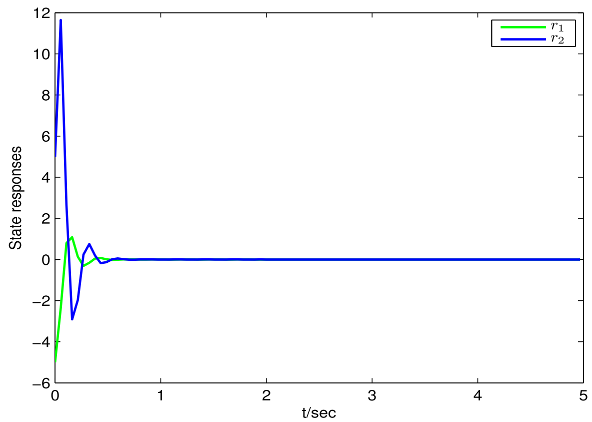

FIGURE 6. State trajectory of the system for Passivity performance in Example 4.1.

the passivity performance. We get the following control gain matrix by employing the MATLAB LMI toolbox to check the LMIs in Theorem 2.

$$\bar{K} = \begin{bmatrix} 0.2832 \; 0.0132 \\ 0.0335 \; 0.0252 \end{bmatrix}.$$

The subsequent simulation is also shown to validate the result obtained from Fig. 6 and Fig. 7. Fig. 6 reflects the resulting state responses under random initial conditions with a distraction $w(t)$. In Fig. 7 demonstrates the performance of the control inputs that converges to zero as well as the passivity performance of both figures is consistent with the available parameters. All of these findings suggest that its designed controller is powerful.

Mixed H_∞ and Passivity performance: $\chi_1 = \tilde{\gamma}^{-1}\alpha I,\ \chi_2 = (1 = \alpha)I,\ \chi_3 = \tilde{\gamma}I,\ \chi_4 = 0$ *and* $\alpha = 0.4$. *At this point, the extended dissipativity performance reduces to the mixed H_∞ and passivity performance. Using MATLAB LMI toolbox and solving LMIs in Theorem 2 helps in acquiring the control gain matrix.*

$$\bar{K} = \begin{bmatrix} 0.0734 \; 0.3121 \\ 0.1521 \; 0.3421 \end{bmatrix}.$$

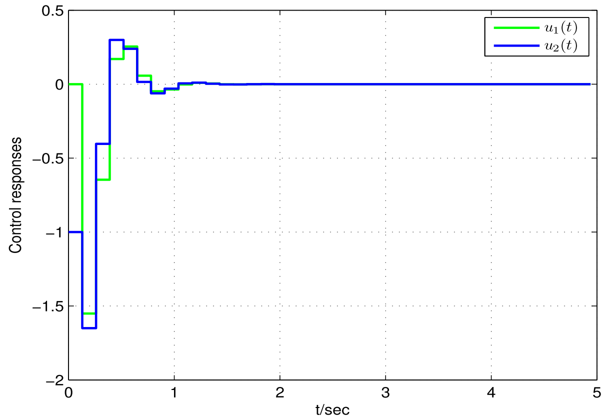

FIGURE 7. Control Response of the system for Passivity performance in Example 4.1.

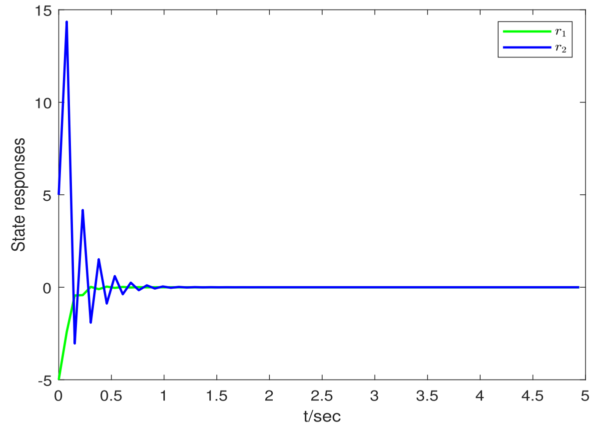

FIGURE 8. State trajectory of the system for Mixed H_∞ and Passivity performance in Example 4.1.

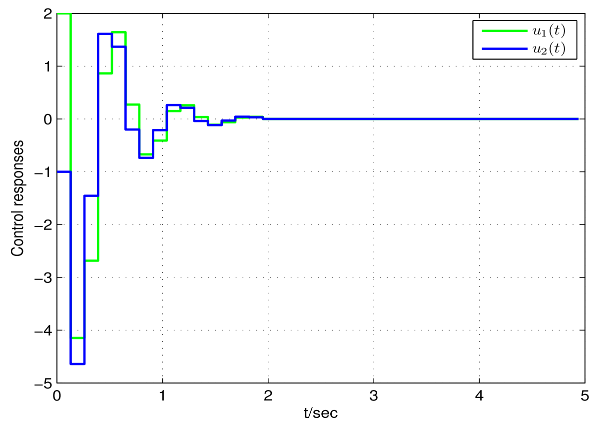

FIGURE 9. Control Response of the system for Mixed H_∞ and Passivity performance in Example 4.1.

With the randomized initial conditions, the dynamical response of the state trajectories and control response of the system (39) has been depicted in Fig. 8 and Fig. 9 and hence shows mixed H_∞ and passivity performance satisfying the above stated parameters. It is possible to obtain that the built controller performs well.

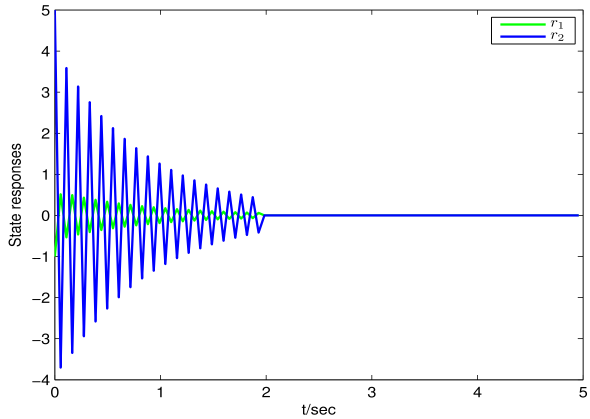

FIGURE 10. State trajectory of the system for $(\mathcal{Q}-\mathcal{S}-\mathcal{R})$ performance in Example 4.1.

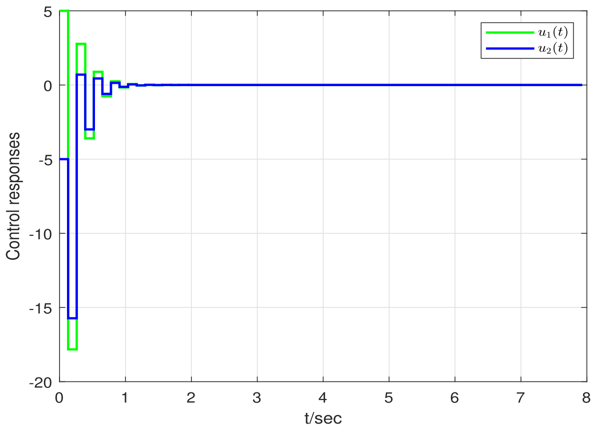

FIGURE 11. Control Response of the system for $(\mathcal{Q}-\mathcal{S}-\mathcal{R})$ performance in Example 4.1.

TABLE 1. Allowable maximum sampling period *h* when $\hat{\tau}_1 = 0.85$.

Results	h	$\hat{\tau}_1$	Gain matrix
[31]	0.24	0.72	$\bar{K} = \begin{bmatrix} -3.9654 & 0.0593 \\ 1.0802 & -4.3424 \end{bmatrix}$
Example 2	0.45	0.85	$\bar{K} = \begin{bmatrix} -3.3261 & 0.0347 \\ 0.5631 & -6.8972 \end{bmatrix}$

$(\mathcal{Q}-\mathcal{S}-\mathcal{R})$ Dissipativity: $\chi_1 = \mathcal{Q},\ \chi_2 = \mathcal{S},\ \chi_3 = \mathcal{R} - \tilde{\alpha} I$, *and* $\chi_4 = 0$ *with*

$$\mathcal{Q} = \begin{bmatrix} -1 & 0 \\ 0 & -1 \end{bmatrix},\ \mathcal{S} = \begin{bmatrix} 0.3 & 0 \\ 0.4 & 0.25 \end{bmatrix},\ \mathcal{R} = \begin{bmatrix} 0.3 & 0 \\ 0 & 0.3 \end{bmatrix}.$$

In the same manner, by solving the LMIs in Theorem 2 and using the above parameters, the following is the gain matrix:

$$\bar{K} = \begin{bmatrix} 5.2126 & 0.0230 \\ 0.0425 & 2.2532 \end{bmatrix},$$

and the dissipativity performance is $\tilde{\alpha} = 0.0072$. *Simultaneously, the relative simulation is demonstrated to verify the obtained result from Fig. 10 and Fig. 11. Fig 10 represents the corresponding state trajectories under the randomized initial condition. In order to explore the simulation results of the controller input* $u(t)$, *the initial condition is taken as* $[-5, 5]^T$. *Then, the control input for the dynamical system (39) has been*

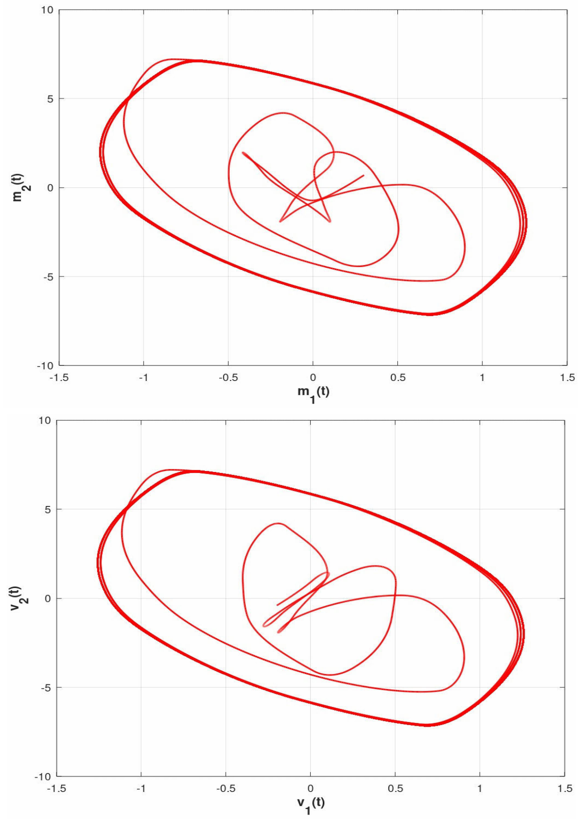

FIGURE 12. Chaotic behaviour of the master and slave system in Example 4.2.

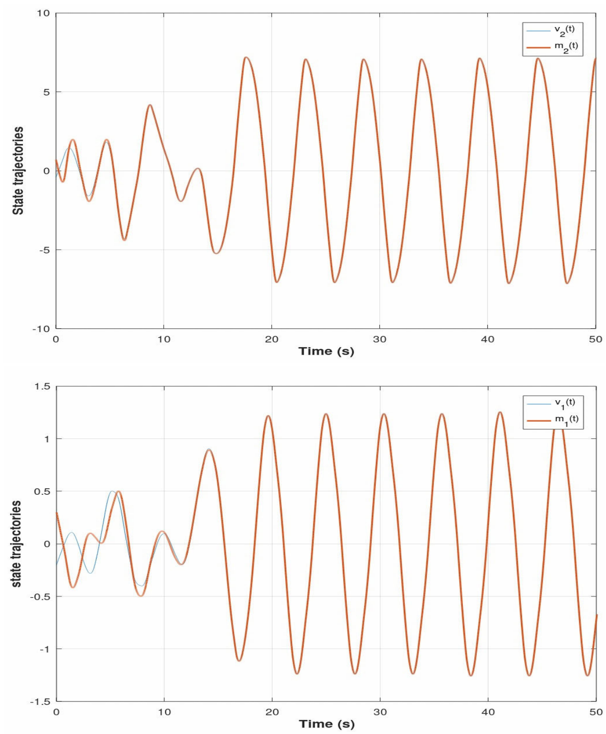

FIGURE 13. State trajectory of the system in Example 4.2.

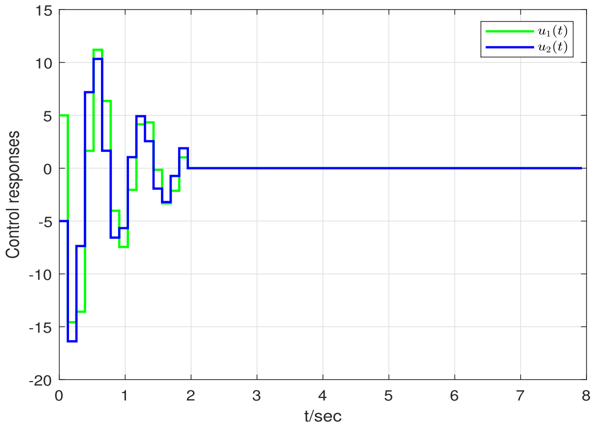

FIGURE 14. Control responses in Example 4.2.

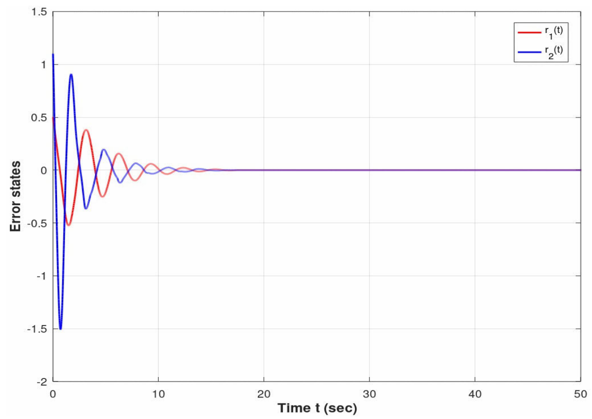

FIGURE 15. Error signals of the system in Example 4.2.

displayed in Fig. 11. Therefore, from the simulation results, we accredit that the state trajectories and the control input converges to zero. Thus, the $(\mathcal{Q}-\mathcal{S}-\mathcal{R})$ *dissipativity performance requirement is satisfied. Therefore, Figs. 2-11 do not only validate the stability region of the system (39), yet the superiorities of our designed controller are also shown.*

Example 2: Consider the following system (40) and choose $0 \leq \hat{\tau}_1(t) \leq \hat{\tau}_1$ *with the parameters as given below:*

$$\begin{aligned} \dot{r}(t) &= -Mr(t) + Cg(r(t)) + W_1 g(r(t-\hat{\tau}_1(t))) + u(t), \\ M &= \begin{bmatrix} 1 & 0 \\ 0 & 0.5 \end{bmatrix}, \; C = \begin{bmatrix} 1.8 & -0.15 \\ -5.2 & 1.5 \end{bmatrix}, \\ W_1 &= \begin{bmatrix} -1.7 & -0.12 \\ -0.26 & -2.5 \end{bmatrix}. \end{aligned} \tag{40}$$

The activation functions are defined to be $g_1(x_1) = g_2(x_2) = tanh(x)$*. The following can then be verified* $s_1^- = s_2^- = 0, s_1^+ = s_2^+ = 1$*. We get the allowable maximum sampling period* $h = 0.45$ *and* $\hat{\tau}_1 = 0.72$ *with the selected parameter values, which is shown in Table 1. By choosing the randomized initial condition, the chaotic oscillator of the master-slave NNs with* $u(t) = 0$ *are given in Fig. 12. The state response of the controlled NNs (40) is depicted in Fig. 13. Furthermore, the response curves of the control input and the error signal are shown in Fig. 14 and Fig. 15. It is evident from Fig. 15 that the error signals approach zero. This implies that the master system synchronizes with the slave system under the considered sampled-data controller.*

V. CONCLUSION

In this paper, the extended dissipativity of RNNs with multiple time-varying delays has been studied via non-fragile sampled-data control. A suitable LKF has been constructed and the results have been derived to prove the quadratically stability and extended dissipativity of RNNs. Finally, non-fragile technique along with the sampled-data controller has been used to synchronize delayed neural networks. The effectiveness of the controller design method has been established by providing suitable simulation results. In the future work, the proposed methods will be extended to many famous dynamical models, such as synchronization of T-S fuzzy NNs, switched Hopfield NNs, memristor NNs, network-based event-triggered control, fractional-order NNs and Markovian jump NNs. This will occur in the near future.

REFERENCES

[1] J. Li, Z. Wang, H. Dong, and G. Ghinea, "Outlier-resistant remote state estimation for recurrent neural networks with mixed time-delays," *IEEE Trans. Neural Netw. Learn. Syst.*, early access, May 18, 2020, doi: 10.1109/TNNLS.2020.2991151.

[2] D. Zhao, Z. Wang, Y. Chen, and G. Wei, "Proportional–Integral observer design for multidelayed sensor-saturated recurrent neural networks: A dynamic event-triggered protocol," *IEEE Trans. Cybern.*, vol. 50, no. 11, pp. 4619–4632, Nov. 2020.

[3] Y. Huang, X. Yuan, H. Long, X. Fan, and T. Cai, "Multistability of fractional-order recurrent neural networks with discontinuous and nonmonotonic activation functions," *IEEE Access*, vol. 7, pp. 116430–116437, 2019.

[4] K. Gu, J. Chen, and V. L. Kharitonov, *Stability of Time-Delay Systems*. Basel, Switzerland: Springer, 2003.

[5] K. Liu, A. Seuret, and Y. Xia, "Stability analysis of systems with time-varying delays via the second-order Bessel–Legendre inequality," *Automatica*, vol. 76, pp. 138–142, Feb. 2017.

[6] K. Gu, "An integral inequality in the stability problem of time-delay systems," in *Proc. 39th IEEE Conf. Decis. Control*, Dec. 2000, pp. 2805–2810.

[7] L. Sun, Y. Tang, W. Wang, and S. Shen, "Stability analysis of time-varying delay neural networks based on new integral inequalities," *J. Franklin Inst.*, vol. 357, no. 15, pp. 10828–10843, Oct. 2020.

[8] N. Gunasekaran, N. M. Thoiyab, P. Muruganantham, G. Rajchakit, and B. Unyong, "Novel results on global robust stability analysis for dynamical delayed neural networks under parameter uncertainties," *IEEE Access*, vol. 8, pp. 178108–178116, 2020.

[9] S. Arik, "Stability analysis of delayed neural networks," *IEEE Trans. Circuits Syst. I, Fundam. Theory Appl.*, vol. 47, no. 7, pp. 1089–1092, Jul. 2000.

[10] H. Zhang, Z. Wang, and D. Liu, "Global asymptotic stability of recurrent neural networks with multiple time-varying delays," *IEEE Trans. Neural Netw.*, vol. 19, no. 5, pp. 855–873, May 2008.

[11] T. Huang, C. Li, S. Duan, and J. A. Starzyk, "Robust exponential stability of uncertain delayed neural networks with stochastic perturbation and impulse effects," *IEEE Trans. Neural Netw. Learn. Syst.*, vol. 23, no. 6, pp. 866–875, Jun. 2012.

[12] Q. Fu, J. Cai, and S. Zhong, "Robust stabilization of memristor-based coupled neural networks with time-varying delays," *Int. J. Control, Autom. Syst.*, vol. 17, no. 10, pp. 2666–2676, Oct. 2019.

[13] F. Kong and Q. Zhu, "Finite-time and fixed-time synchronization criteria for discontinuous fuzzy neural networks of neutral-type in Hale's form," *IEEE Access*, vol. 7, pp. 99842–99855, 2019.

[14] Y. Chen, Z. Wang, B. Shen, and H. Dong, "Exponential synchronization for delayed dynamical networks via intermittent control: Dealing with actuator saturations," *IEEE Trans. Neural Netw. Learn. Syst.*, vol. 30, no. 4, pp. 1000–1012, Apr. 2019.

[15] R. Vadivel, M. S. Ali, and Y. H. Joo, "Drive-response synchronization of uncertain Markov jump generalized neural networks with interval time varying delays via decentralized event-triggered communication scheme," *J. Franklin Inst.*, vol. 357, no. 11, pp. 6824–6857, Jul. 2020.
[16] J. Li, H. Dong, Z. Wang, and X. Bu, "Partial-neurons-based passivity-guaranteed state estimation for neural networks with randomly occurring time delays," *IEEE Trans. Neural Netw. Learn. Syst.*, vol. 31, no. 9, pp. 3747–3753, Sep. 2020.
[17] K. Zhong, S. Zhu, and Q. Yang, "Dissipativity results for memristor-based recurrent neural networks with mixed delays," in *Proc. 6th Int. Conf. Intell. Control Inf. Process. (ICICIP)*, Nov. 2015, pp. 406–411.
[18] Q. Fu, J. Cai, S. Zhong, and Y. Yu, "Dissipativity and passivity analysis for memristor-based neural networks with leakage and two additive time-varying delays," *Neurocomputing*, vol. 275, pp. 747–757, Jan. 2018.
[19] J. Cao, K. Yuan, and H.-X. Li, "Global asymptotical stability of recurrent neural networks with multiple discrete delays and distributed delays," *IEEE Trans. Neural Netw.*, vol. 17, no. 6, pp. 1646–1651, Nov. 2006.
[20] X. Liang, J. Xia, G. Chen, H. Shen, and Z. Wang, "Sampled-data control for fuzzy Markovian jump systems with actuator saturation," *IEEE Access*, vol. 7, pp. 180417–180427, 2019.
[21] N. Gunasekaran, R. Saravanakumar, Y. H. Joo, and H. S. Kim, "Finite-time synchronization of sampled-data T–S fuzzy complex dynamical networks subject to average dwell-time approach," *Fuzzy Sets Syst.*, vol. 374, pp. 40–59, Nov. 2019.
[22] H. R. Karimi and H. Gao, "New delay-dependent exponential H_∞ synchronization for uncertain neural networks with mixed time delays," *IEEE Trans. Syst., Man, Cybern. B, Cybern.)*, vol. 40, no. 1, pp. 173–185, Feb. 2010.
[23] J. Hu, Z. Wang, H. Gao, and L. K. Stergioulas, "Robust sliding mode control for discrete stochastic systems with mixed time delays, randomly occurring uncertainties, and randomly occurring nonlinearities," *IEEE Trans. Ind. Electron.*, vol. 59, no. 7, pp. 3008–3015, Jul. 2012.
[24] Q. Fu, S. Zhong, W. Jiang, and W. Xie, "Projective synchronization of fuzzy memristive neural networks with pinning impulsive control," *J. Franklin Inst.*, vol. 357, no. 15, pp. 10387–10409, Oct. 2020.
[25] N. Gunasekaran, G. Zhai, and Q. Yu, "Sampled-data synchronization of delayed multi-agent networks and its application to coupled circuit," *Neurocomputing*, vol. 413, pp. 499–511, Nov. 2020.
[26] J. Luo, M. Li, X. Liu, W. Tian, S. Zhong, and K. Shi, "Stabilization analysis for fuzzy systems with a switched sampled-data control," *J. Franklin Inst.*, vol. 357, no. 1, pp. 39–58, 2020.
[27] K. Shi, J. Wang, Y. Tang, and S. Zhong, "Reliable asynchronous sampled-data filtering of T–S fuzzy uncertain delayed neural networks with stochastic switched topologies," *Fuzzy Sets Syst.*, vol. 381, pp. 1–25, Feb. 2020.
[28] B. Brogliato, R. Lozano, B. Maschke, and O. Egeland, "Dissipative systems analysis and control," in *Theory and Applications*, vol. 2. Springer, 2007.
[29] H. Wei, R. Li, C. Chen, and Z. Tu, "Extended dissipative analysis for memristive neural networks with two additive time-varying delay components," *Neurocomputing*, vol. 216, pp. 429–438, Dec. 2016.
[30] K. Shi, J. Wang, S. Zhong, Y. Tang, and J. Cheng, "Non-fragile memory filtering of T-S fuzzy delayed neural networks based on switched fuzzy sampled-data control," *Fuzzy Sets Syst.*, vol. 394, pp. 40–64, Sep. 2020.
[31] S.-P. Xiao, H.-H. Lian, K. L. Teo, H.-B. Zeng, and X.-H. Zhang, "A new Lyapunov functional approach to sampled-data synchronization control for delayed neural networks," *J. Franklin Inst.*, vol. 355, no. 17, pp. 8857–8873, Nov. 2018.

R. ANBUVITHYA received the B.Sc. degree in mathematics from Holy Cross College, Tiruchirappalli, India, which is affiliated to Bharathidasan University, in 2007, the M.Sc. and M.Phil. degrees from the Department of Mathematics, Periyar University, Salem, India, in 2010 and 2011, respectively, and the Ph.D. degree under the guidance of Dr. P. Prakash. She is an Associate Professor of Mathematics with Periyar University, in 2016. She served as an Ad-Hoc Faculty with the Department of Mathematics, National Institute of Technology, Tiruchirappalli, from July 2015 to July 2016. She is currently working as an Assistant Professor with the Department of Mathematics, Sri Sarada College for Women (Autonomous), Salem. Her current research interests include stability analysis of neural networks, delay differential systems, and robust control for nonlinear systems.

S. DHEEPIKA SRI received the B.Sc. and M.Sc. degrees in mathematics from Sri Sarada College for Women (Autonomous), Salem, India, in 2017 and 2019, respectively, where she is currently pursuing the M.Phil. degree with the Department of Mathematics. Her current research interests include neural networks, delay differential systems, and mathematical modeling.

R. VADIVEL received the B.Sc., M.Sc., and M.Phil. degrees in mathematics from the Sri Ramakrishna Mission Vidyalaya College of Arts and Science affiliated to Bharathiar University, Coimbatore, India, in 2007, 2010, and 2012, respectively, and the Ph.D. degree from the Department of Mathematics, Thiruvalluvar University, Vellore, India, in 2018. He was a Postdoctoral Research Fellow with the Research Center for Wind Energy Systems, Kunsan National University, Gunsan, South Korea, from 2018 to 2019. He is currently working as a Lecturer with the Department of Mathematics, Faculty of Science and Technology, Phuket Rajabhat University, Thailand.

NALLAPPAN GUNASEKARAN received the B.Sc. degree from Mahendra Arts and Science College, Periyar University, Salem, India, in 2009, the master's degree from Jamal Mohamed College affiliated to Bharathidasan University, Trichy, India, in 2012, the M.Phil. degree from Bharathidasan University, in 2013, and the Ph.D. degree in mathematics from Thiruvalluvar University, Vellore, India, in 2018. He was a Postdoctoral Research Fellow with the Research Center for Wind Energy Systems, Kunsan National University, Gunsan, South Korea, from 2017 to 2018. He is currently working as a Postdoctoral Research Fellow with the Computational Intelligence Laboratory, Department of Advanced Science and Technology, Toyota Technological Institute, Nagoya, Japan. He has authored and coauthored of more than 30 research articles in various SCI journals. His research interests include complex-valued NNs, complex dynamical networks, control theory, stability analysis, sampled-data control, multi-agent systems, T-S fuzzy theory, and cryptography. He serves as a Reviewer for various SCI journals.

PORPATTAMA HAMMACHUKIATTIKUL received the Ph.D. degree in applied mathematics from the King Mongkut's University of Technology Thonburi (KMUTT), Bangkok, Thailand. She is currently working with the Department of Mathematics, Phuket Rajabhat University (PKRU), Phuket, Thailand. Her research interests include mathematic model, climate change, atmospheric model, Lyapunov theory, neural networks, stability analysis of dynamical systems, synchronization, and chaos theory.